Available online at www.sciencedirect.com
ScienceDirect
Journal of Power Sources 171 (2007) 738–746
JOURNAL OF POWER SOURCES
www.elsevier.com/locate/jpowsour

Numerical investigation of transient responses of a PEM fuel cell using a two-phase non-isothermal mixed-domain model

Hua Meng *

Center for Engineering and Scientific Computation, School of Aeronautics and Astronautics, P.O. Box 1455, Zhejiang University, Hangzhou, Zhejiang 310027, PR China

Received 15 May 2007; received in revised form 10 June 2007; accepted 11 June 2007
Available online 21 June 2007

Abstract

In this paper, a transient two-phase non-isothermal PEM fuel cell model has been developed based on the previously established two-phase mixed-domain approach. This model is capable of solving two-phase flow and heat transfer processes simultaneously and has been applied herein for two-dimensional time-accurate simulations to fully examine the effects of liquid water transport and heat transfer phenomena on the transient responses of a PEM fuel cell undergoing a step change of cell voltage, with and without condensation/evaporation interfaces. The present numerical results show that under isothermal two-phase conditions, the presence of liquid water in the porous materials increases the current density over-shoot and under-shoot, while under the non-isothermal two-phase conditions, the heat transfer process significantly increases the transient response time. The present studies also indicate that proper consideration of the liquid droplet coverage at the GDL/GC interface results in the increased liquid saturation values inside the porous materials and consequently the drastically increased over-shoot and under-shoot of the current density. In fact, the transient characteristics of the interfacial liquid droplet coverage could exert influences on not only the magnitude but also the time of the transient response process.

Keywords: PEM fuel cell; Transient response; Dynamic analysis; Two-phase model; Thermal management; Water management

1. Introduction

Numerical modeling and simulation of PEM fuel cells is crucial for revealing the underlying physics and facilitating cell design and optimization. Many PEM fuel cell models have been developed to achieve these goals, including the single-phase or pseudo single-phase PEM fuel cell models [1–13], which either do not account for liquid water transport phenomena or simplify its treatment, and the two-phase models [14–26], which handle the liquid water transport and the related phenomena explicitly. The majority of these models, however, consider only steady-state operation conditions of PEM fuel cells. Since a PEM fuel cell would experience start-up and shut-down processes and frequent load changes for automotive applications, a numerical model capable of investigating transient responses is thus needed.

A transient PEM fuel cell model was developed in the work of Um et al. [1], but the main studies were not focused on the transient analysis, and thus only a preliminary result concerning the cell dynamic response with a step change of cell voltage was presented. This work was further extended by Wang and Wang [27] into a transient three-dimensional single-phase isothermal PEM fuel cell model. They estimated three time constants concerning electrochemical double-layer charging/discharging, gas transport, and membrane hydration/dehydration processes, and concluded that the double-layer charging/discharging process was very fast and could thus be safely neglected in transient analyses of PEM fuel cell operations. They also conducted extensive numerical simulations with step changes of cell voltage and inlet humidity and discussed the dynamic physics of the transient phenomena. Wang and Wang [28] later studied the dynamic responses of a PEM fuel cell undergoing a step change of current based on the work of Meng and Wang [5,29] with a proper account of the electron transport. Shimpalee et al. [30,31] numerically simulated the transient responses of a PEM fuel cell subjected to variable load changes based on a three-dimensional

* Tel.: +86 571 87953166; fax: +86 571 87953167.
E-mail address: menghua@zju.edu.cn.

0378-7753/$ – see front matter © 2007 Elsevier B.V. All rights reserved.
doi:10.1016/j.jpowsour.2007.06.029

Nomenclature

a	water activity or stoichiometry coefficient
c	molar concentration (mol m^{-3})
C_p	constant-pressure heat capacity (J kg^{-1} K^{-1})
D	mass diffusivity (m^2 s^{-1})
D_λ	water content diffusivity (mol m^{-1} s^{-1})
EW	equivalent weight of the membrane (kg mol^{-1})
F	Faraday constant (96,487 C mol^{-1})
j	transfer current density (A m^{-3})
k	thermal conductivity (W m^{-1} K^{-1})
K	permeability (m^2)
n_d	electro-osmotic drag coefficient
p	gas-phase pressure (Pa)
p_c	capillary pressure (Pa)
R_u	universal gas constant (J mol^{-1} K^{-1})
s	liquid saturation
S	source term
t	time (s)
T	temperature (K)
u	gas-phase velocity (m s^{-1})
U_0	open-circuit potential (V)
V_{cell}	cell voltage (V)
W	molecular weight (kg mol^{-1})

Greek letters

ε	porosity
ε_m	fraction of the membrane phase in the catalyst layer
η	over-potential (V)
κ	proton conductivity (S m^{-1})
λ	water content
μ	viscosity (kg m^{-1} s^{-1})
θ_c	contact angle
ρ	gaseous density (kg m^{-3})
σ	electronic conductivity (S m^{-1}) or surface tension (N m^{-1})
τ	viscous stress tensor
ϕ	phase potential (V)

Superscripts

cl	catalyst layer
eff	effective value
l	liquid phase
sat	saturation value
v	vapor phase

Subscripts

cl	catalyst layer
e	electrolyte or energy
g	gaseous phase
i	species
l	liquid
m	membrane
s	electron or solid phase
sat	saturation value
w	water

single-phase isothermal PEM fuel cell model. The simulations were conducted for a PEM fuel cell with a serpentine flow-field and a 10 cm^2 reactive area. They presented numerical results under excess, normal, and minimal fuel and air supplies. Recently, Wu et al. [32] developed a transient two-dimensional single-phase non-isothermal model of PEM fuel cells, and with an inclusion of the heat transfer equation, they were able to consider four transient processes, namely the electrochemical double-layer charging/discharging, species transport, membrane hydration/dehydration, and heat transfer processes. Based on their numerical results, they concluded that the heat transfer process could exert significant influences on fuel cell dynamic responses.

The transient PEM fuel cell models briefly reviewed in the early section are all based on single-phase or pseudo single-phase simplifications. Wu et al. [33] have attempted to consider the liquid water effect by defining a fixed liquid saturation of 10% in the porous materials in a PEM fuel cell based on the two-phase results provided in the review paper of Wang [34]. Natarajan and Nguyen [21] developed a transient two-dimensional two-phase model for the cathode of a PEM fuel cell, and they concluded that liquid water transport would prolong the cell response time, especially under the current-collecting land. This work only considered the cathode side under isothermal conditions. Since the inclusion of the temperature effect is crucial for correctly simulating the condensation/evaporation phenomena in two-phase flows, Shah et al. [35] recently developed a transient non-isothermal model for a PEM fuel cell. They presented numerical results in the form of potential sweeps and were able to quantitatively predict the hysteresis phenomenon often observed in PEM fuel cell experiments. However, the model is one-dimensional and thus could not be applied to fully investigate the complex multi-dimensional physics in practical PEM fuel cell operations. Song et al. [36] also developed a transient one-dimensional non-isothermal two-phase PEM fuel cell model to investigate transient liquid water transport in the cathode GDL. The phase change phenomenon and parameters affecting transient and steady-state liquid water transport were discussed.

In order to fully investigate the dynamic responses of a PEM fuel cell under practical operation conditions and further enhance fundamental understandings of the intricate interactions of thermal and water managements during the cell transient operations, a transient two-phase non-isothermal PEM fuel cell model is developed in the present paper based on a previously established two-phase mixed-domain approach [26]. The model is capable of solving two-phase flow and heat transfer processes simultaneously with a proper consideration of the effect of liquid droplet coverage at the gas diffusion layer (GDL) and the gas channel (GC) interface. The model will be applied herein for two-dimensional time-accurate simulations in a cross-section perpendicular to the flow direction so that the effects of liquid water transport and heat transfer phenomena on the transient responses of a PEM fuel cell, with and without condensation/evaporation interfaces, could be fully examined and clearly presented.

2. Theoretical formulation

The complete conservation equations in their transient forms are developed in this paper based on a previously established steady-state multi-dimensional two-phase mixed-domain PEM fuel cell model [26]. First, the transient conservation equations of mass, momentum, species concentrations in the gaseous phase are presented.

Mass conservation:

$$\frac{\partial[\varepsilon(1-s)\rho]}{\partial t} + \nabla\cdot(\rho\vec{u}) = 0 \tag{1}$$

Momentum conservation:

$$\frac{1}{\varepsilon(1-s)}\frac{\partial(\rho\vec{u})}{\partial t} + \frac{1}{\varepsilon^2(1-s)^2}\nabla\cdot(\rho\vec{u}\vec{u}) = -\nabla p + \nabla\cdot\tau + S_{\mathrm{u}} \tag{2}$$

Species conservation:

$$\frac{\partial[\varepsilon^{\mathrm{eff}}(1-s)c_i]}{\partial t} + \nabla\cdot(\vec{u}c_i) = \nabla\cdot(D_i^{\mathrm{eff}}\nabla c_i) + S_i \tag{3}$$

In Eq. (3), based on the mixed-domain approach [12,13], the water vapor concentration is solved only in the gas channels, gas diffusion layers, and catalyst layers on both the anode and cathode sides. In the two catalyst layers, the dissolved water phase (water in the membrane phase) is assumed to be in thermodynamic phase equilibrium with water vapor, and its transport process is combined into the water vapor transport equation using the following water diffusivity [12,13]:

$$D_{\mathrm{w}}^{\mathrm{cl}} = \varepsilon_{\mathrm{cl}}^{1.5} D_{\mathrm{w}}^{\mathrm{cl,g}} + \varepsilon_{\mathrm{m}}^{1.5} D_\lambda \frac{R_{\mathrm{u}}T}{p_{\mathrm{sat}}}\frac{\mathrm{d}\lambda}{\mathrm{d}a} \tag{4}$$

In addition, the effective porosity, $\varepsilon^{\mathrm{eff}}$, in the water transport equation should be modified as [27,32]

$$\varepsilon^{\mathrm{eff}} = \varepsilon + \frac{\varepsilon_{\mathrm{m}}}{1-s}\frac{R_{\mathrm{u}}T}{p_{\mathrm{sat}}}\frac{\mathrm{d}\lambda}{\mathrm{d}a} \tag{5}$$

In other species transport equations, the effective porosity remains as

$$\varepsilon^{\mathrm{eff}} = \varepsilon \tag{6}$$

Considering the liquid water effect, the effective gaseous species diffusion coefficients should be further modified as

$$D_i^{\mathrm{eff}} = D_i(1-s)^{1.5} \tag{7}$$

In the present two-phase model, water produced in the cathode catalyst layer is assumed to be in vapor phase or dissolved phase [26], as they are at thermodynamic equilibrium. Although the thermodynamic equilibrium condition is a common assumption also made in many prior transient numerical models [27,28,32,33], its validity in transient simulations requires further verification.

In this transient two-phase model, liquid water transport is taken into account using the traditional two-fluid method. As discussed in [26], we will ensure the states of water vapor (or the dissolved water phase in the catalyst layers) and liquid water closely approach their thermodynamic equilibrium conditions by choosing appropriate condensation and evaporation rate coefficients. It should also be emphasized that the validity of this assumption needs further investigation for transient simulations.

The transient conservation equations of liquid water transport are presented next.

Liquid mass conservation:

$$\frac{\partial(\varepsilon\rho_{\mathrm{l}}s)}{\partial t} + \nabla\cdot(\rho_{\mathrm{l}}\vec{u}_{\mathrm{l}}) = S_{\mathrm{vl}}W_{\mathrm{w}} \tag{8}$$

where an expression for the condensation/evaporation rate can be found in [26]. In the porous materials, based on the Darcy's law, the liquid water velocity is derived as

$$\vec{u}_{\mathrm{l}} = -\frac{K_{\mathrm{rl}}K}{\mu^{\mathrm{l}}}\nabla p^{\mathrm{l}} \tag{9}$$

where the liquid pressure is defined as [14]

$$p^{\mathrm{l}} = p - p_{\mathrm{c}} \tag{10}$$

Eqs. (8)–(10) can be combined to produce a transient conservation equation for the liquid saturation, which is

$$\frac{\partial(\varepsilon\rho_{\mathrm{l}}s)}{\partial t} + \nabla\cdot\left[\frac{\rho_{\mathrm{l}}K_{\mathrm{rl}}K}{\mu^{\mathrm{l}}}\frac{\partial p_{\mathrm{c}}}{\partial s}\nabla s\right] - \nabla\cdot\left[\frac{\rho_{\mathrm{l}}K_{\mathrm{rl}}K}{\mu^{\mathrm{l}}}\nabla p\right] = S_{\mathrm{vl}}W_{\mathrm{w}} \tag{11}$$

The transient water content conservation equation inside the membrane is in the following form:

$$\frac{\partial}{\partial t}\left(\frac{\rho_{\mathrm{m}}\lambda}{\mathrm{EW}}\right) = \nabla\cdot(D_\lambda\nabla\lambda) + S_\lambda \tag{12}$$

The transient conservation equation of energy is derived as

$$\frac{\partial}{\partial t}[(\rho C_p)^{\mathrm{eff}}T] + \nabla\cdot(\rho C_p\vec{u}T) + \nabla\cdot(\rho_{\mathrm{l}}C_{p,\mathrm{l}}\vec{u}_{\mathrm{l}}T) = \nabla\cdot(k^{\mathrm{eff}}\nabla T) + S_{\mathrm{T}} \tag{13}$$

where the effective parameter, $(\rho C_p)^{\mathrm{eff}}$, can be determined in the following general form:

$$(\rho C_p)^{\mathrm{eff}} = \varepsilon(1-s)\rho C_p + \varepsilon s(\rho C_p)_{\mathrm{l}} + (1-\varepsilon-\varepsilon_{\mathrm{m}})(\rho C_p)_{\mathrm{s}} + \varepsilon_{\mathrm{m}}(\rho C_p)_{\mathrm{m}} \tag{14}$$

The related parameters are provided in Table 1. The effective thermal conductivity of each cell layer is approximated as a constant in the present numerical studies and is also listed in Table 1. It should be noted that, in this paper, specific heat capacity, C_p, of the membrane material has been substituted with that of PTFE, since it is not available in the open literature, as also discussed in [32].

Finally, the conservation equations of proton and electron transport are derived as

Proton transport:

$$\nabla\cdot(\kappa^{\mathrm{eff}}\nabla\phi_{\mathrm{e}}) + S_{\mathrm{e}} = 0 \tag{15}$$

Table 1
Physicochemical parameters

Anode volumetric exchange current density, aj_0 (A m^{-3})	1.0E+9
Cathode volumetric exchange current density, aj_0 (A m^{-3})	1.0E+4
Reference hydrogen concentration, C_{H_2} (mol m^{-3})	40
Reference oxygen concentration, C_{O_2} (mol m^{-3})	40
Anode transfer coefficients	$\alpha_a = \alpha_c = 1$
Cathode transfer coefficient	$\alpha_c = 1$
Faraday constant, F (C mol^{-1})	96,487
GDL porosity	0.6
Porosity of catalyst layer	0.12
Volume fraction of ionomer in catalyst layer	0.4
GDL permeability (m^2)	1.0E−12
Catalyst layer permeability (m^2)	1.0E−13
Equivalent weight of ionomer (kg mol^{-1})	1.1
Dry membrane density (kg m^{-3})	1980
Effective electronic conductivity in CL/GDL (S m^{-1})	5000
Operation pressure (atm)	2
Condensation rate coefficient (s^{-1}) [26]	5000
Evaporation rate coefficient (s^{-1} Pa^{-1}) [26]	1.0E−4
Liquid water density (kg m^{-3})	1000
Liquid water viscosity (N s m^{-2})	3.5E−4
Surface tension (N m^{-1})	6.25E−2
Contact angle in GDL	110
Contact angle in CL	95
Thermal conductivity of GDL (W m^{-1} K^{-1}) [26]	1.5
Thermal conductivity of CL (W m^{-1} K^{-1}) [26]	1.5
Thermal conductivity of the membrane (W m^{-1} K^{-1}) [26]	0.5
Heat of vaporization (J kg^{-1})	2.3E+6
Density of carbon material (kg m^{-3}) [32]	2200
Heat capacity of carbon material (J kg^{-1} K^{-1}) [32]	1050
Heat capacity of liquid water (J kg^{-1} K^{-1}) [32]	4200
Heat capacity of membrane material (J kg^{-1} K^{-1}) [32]	1050

Electron transport:

$$\nabla \cdot (\sigma^{\text{eff}} \nabla \phi_s) + S_s = 0 \tag{16}$$

Based on the theoretical analyses in [27,33], since the electrochemical double-layer charging/discharging process is very fast, the transient terms in the two equations can be safely neglected and the two equations thus remain in the steady-state form.

The relevant expressions for the source terms and the other physicochemical relationships can be found in Table 2 and the reference [26].

The conservation equations, Eqs. (1)–(3), (11)–(13), (15) and (16), constitute the present transient two-phase non-isothermal PEM fuel cell model. This model is applied for numerical simulations in a two-dimensional configuration to fully examine the effects of liquid water transport and heat transfer phenomena on the transient responses of a PEM fuel cell. The computational domain includes five regions, namely the gas diffusion layers and catalyst layers on both the anode and cathode sides, and the membrane. In the present two-dimensional simulation, since fluid flows in gas channels are neglected, the gaseous velocity and pressure are not computed. This simplification is valid based on the theoretical and numerical analyses of the Peclet number in the porous materials in [13,37]. Therefore, the conservation equations, Eqs. (3), (11)–(13), (15) and (16), are actually solved in the present two-dimensional simulations.

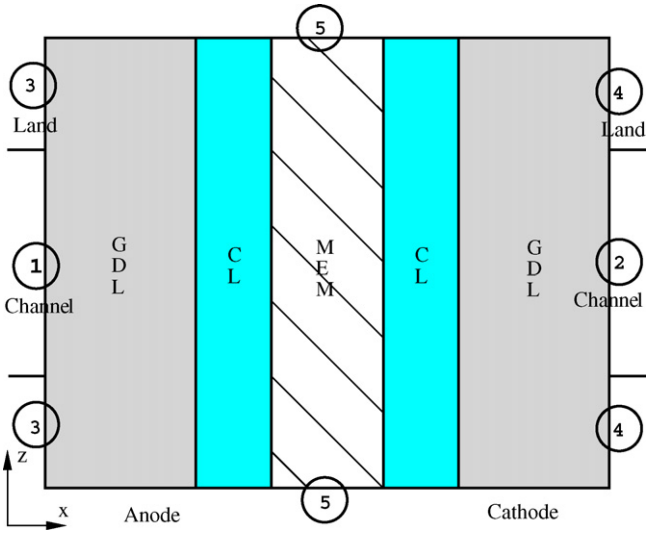

Fig. 1. Cell geometry and the related boundaries.

There are five boundary conditions to be specified, as shown in Fig. 1. The details regarding these boundary conditions can be found in [26] and are thus not repeated in this paper.

The present numerical studies will focus on the transient responses of a PEM fuel cell with a step change of cell voltage under various operation conditions, i.e. single-phase versus two-phase and isothermal versus non-isothermal. The initial conditions are defined as the steady-state numerical solutions at the previous cell voltage.

3. Result and discussion

The present transient two-phase non-isothermal PEM fuel cell model has been implemented into a commercial CFD package, Fluent, through its user coding capabilities and applied herein for two-dimensional numerical simulations, as shown in Fig. 1. The geometric parameters of the fuel cell are listed in Table 3.

Hydrogen and water vapor is fed into the anode while air and water vapor into the cathode. The fuel cell is operated at 2 atm on both the anode and cathode sides. The cell stoichiometry number is two on both sides with a reference current density of 1 A cm^{-2}. For all the calculations carried out in this paper, the boundary temperature is fixed at 80 °C. In order to investigate the effects of two-phase flows and liquid water flooding on the transient responses of the fuel cell, the inlet gas mixtures are set as fully humidified at an inlet temperature of 80 °C on both sides. Based on these operation conditions, the inlet species concentrations can be easily determined and specified at boundaries 1 and 2. Therefore, the present transient two-dimensional numerical calculations simulate a cross-section perpendicular to the flow direction at the inlet of a PEM fuel cell.

Careful grid independence study has been conducted in [26], and a total of 1600 computational cells have been used in the present simulations. In order to obtain time-accurate solutions, variable time steps have been used in the present calculations. The time step is initially very small, 0.01 s, in order to cap-

Table 2
Electrochemical and physical relationships

Description	Expression
Transfer current density ($A\,m^{-3}$)	$j = aj_{0,a}^{\mathrm{ref}}\left(\frac{c_{H_2}}{c_{H_2,\mathrm{ref}}}\right)^{1/2}\left(\frac{\alpha_a+\alpha_c}{RT}\cdot F\cdot\eta\right)$, in anode side
	$j = aj_{0,c}^{\mathrm{ref}}\left(\frac{c_{O_2}}{c_{O_2,\mathrm{ref}}}\right)\exp\left(-\frac{\alpha_c}{RT}\cdot F\cdot\eta\right)$, in cathode side
Over-potential (V)	$\eta = \phi_s - \phi_e$, in anode side $\eta = \phi_s - \phi_e - U_o$, in cathode side
Open-circuit potential (V)	$U_0 = 1.23 - 0.9\times10^{-3}(T-298)$
Electro-osmotic drag coefficient	$n_d = \begin{cases} 1.0, & \text{for } \lambda \le 14 \\ \frac{1.5}{8}(\lambda-14)+1.0, & \text{otherwise} \end{cases}$
Water activity	$a = \frac{C_w R_u T}{p^{\mathrm{sat}}}$
Water saturation pressure (atm)	$\log_{10} p^{\mathrm{sat}} = -2.1794 + 0.02953(T-273.15) - 9.1837\times10^{-5}(T-273.15)^2 + 1.4454\times10^{-7}(T-273.15)^3$
Partial pressure of water vapor (Pa)	$p^{v} = C_w R_u T$
Membrane water diffusivity ($m^2\,s^{-1}$)	$D_w^m = \begin{cases} 3.1\times10^{-7}\lambda(e^{0.28\lambda}-1)\cdot e^{[-2346/T]}, & 0<\lambda\le3 \\ 4.17\times10^{-8}\lambda(1+161\,e^{-\lambda})\cdot e^{[-2346/T]}, & \text{otherwise} \end{cases}$
Water content diffusivity ($mol\,m^{-1}\,s^{-1}$)	$D_\lambda = \frac{\rho_m}{EW} D_w^m$
Proton conductivity ($S\,m^{-1}$)	$\kappa = (0.5139\lambda - 0.326)\exp\left[1268\left(\frac{1}{303}-\frac{1}{T}\right)\right]$

ture the initial rapid variations, and it increases gradually as the calculations progress.

The transient responses of the PEM fuel cell corresponding to a step change of cell voltage are first studied under both single-phase and two-phase isothermal conditions. In the two-phase calculations, the liquid droplet coverage phenomenon at the gas diffusion layer (GDL) and gas channel (GC) interface is temporarily neglected, meaning that s_{int} on the cathode side is set as zero. The effects of the liquid droplet coverage at the GDL/GC interface on the cathode side will be discussed in detail later in this section.

Fig. 2 compares the dynamic responses of the fuel cell with a step decrease of cell voltage from 0.75 to 0.65 V under both single- and two-phase conditions. Since the contact resistances from the electron transport process are neglected in the calculations, the cell performs much better than it could in real-world operations, but this should not affect the present numerical studies. Results in Fig. 2 clearly indicate that under the two-phase condition, although the dynamic response time does not change, the magnitude of the current density over-shoot increases, comparing to that under the single-phase condition. As discussed in [27,32], the magnitude of the current density over-shoot results from the initial richer oxygen concentration maintained at a higher cell voltage of 0.75 V. Under the two-phase condition, with the decrease of the cell voltage and consequently the increase of the current density, the liquid saturation value increases as well, eventually rendering less oxygen reaching the catalyst layer at the steady-state and thus increasing current density over-shoot.

Fig. 3 displays variations of the oxygen concentration in the cathode catalyst layer at different time steps under the two-phase condition. The results indicate that the oxygen concentration changes dramatically from 0 to 0.25 s, but after that, it stabi-

Table 3
Cell geometric parameters

Fuel cell geometry [mm]	
Layer thickness	
Diffusion	0.3
Catalyst	0.01
Membrane	0.025
Land width	0.5
Channel width	1.0
Computational cell numbers	~1600

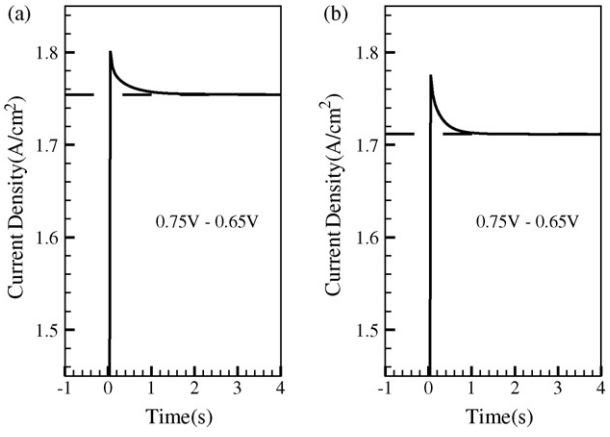

Fig. 2. Transient responses of the fuel cell with a step decrease of cell voltage under (a) single-phase and (b) two-phase isothermal conditions.

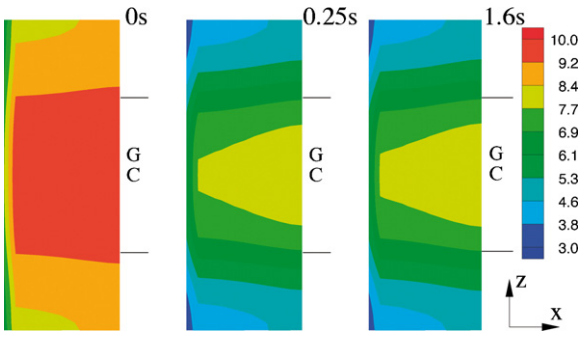

Fig. 3. Transient variations of the oxygen concentration in the cathode catalyst layer corresponding to the same operation condition as in Fig. 2b.

lizes inside the cathode catalyst layer. This clearly indicates that the oxygen concentration dictates the magnitude of the current density over-shoot but not the dynamic response time. In fact, the dynamic response time is controlled by the membrane hydration/dehydration process, as manifested in Fig. 4, which displays the transient variations of the water content inside the membrane under the two-phase condition. With the decrease of the cell voltage from 0.75 to 0.65 V, the current density increases, and as such the electro-osmotic drag increases as well, causing larger water content gradient inside the membrane. The water content inside the membrane varies from 0 to 1.6 s, consistent with the cell dynamic response time.

Fig. 5 compares the dynamic responses of the fuel cell with a step increase of cell voltage from 0.65 to 0.75 V under both single- and two-phase conditions. Now the current density experiences under-shoot initially under both conditions, dictated by the low oxygen concentration initially maintained at the cell voltage of 0.65 V. Because of the presence of liquid water, the magnitude of the current density under-shoot is slightly stronger under the two-phase condition than that under the single-phase condition. In addition, the results in Figs. 2 and 5 indicate that the cell response time is less than 2 s with a step change of cell voltage under both the single- and two-phase conditions. This further verifies that using a thin membrane would reduce the transient response time of a PEM fuel cell, a conclusion consistent with the results in reference [32] calculated using a single-phase model.

The effect of heat transfer process on the transient response of a PEM fuel cell is further examined under the two-phase

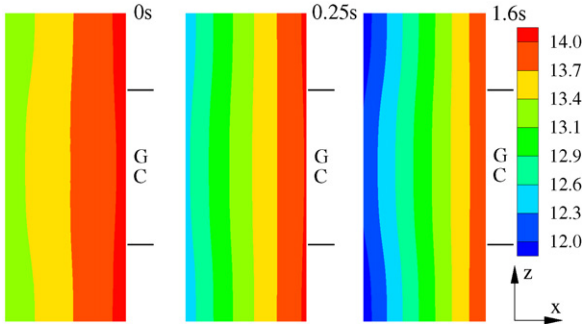

Fig. 4. Transient variations of water content inside the membrane corresponding to the same operation condition as in Fig. 2b.

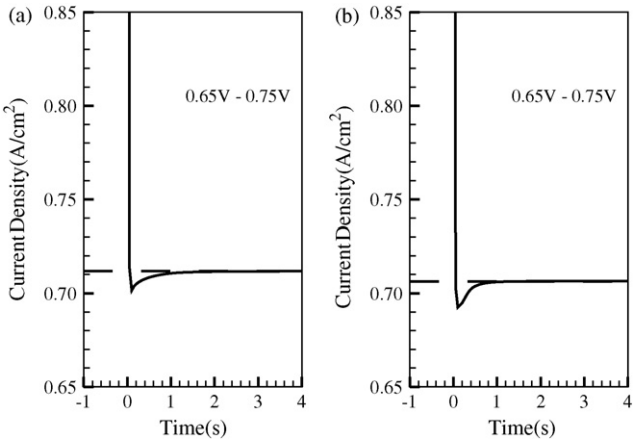

Fig. 5. Transient responses of the fuel cell with a step increase of cell voltage under (a) single-phase and (b) two-phase isothermal conditions.

condition in Fig. 6, which compares the transient variations of the current density with a step decrease of cell voltage from 0.75 to 0.65 V under both isothermal and non-isothermal conditions. Although under the non-isothermal two-phase condition, the magnitude of the current density over-shoot only increases slightly, the response time of the fuel cell increases dramatically, from around 1.6 s under the isothermal condition to around 8 s under the non-isothermal condition. The same conclusion can be drawn from Fig. 7, which compares the transient responses of the current density with a step increase of cell voltage from 0.65 to 0.75 V under both isothermal and non-isothermal two-phase conditions. In addition, under both isothermal and non-isothermal two-phase conditions, the transient response time with a step decrease of cell voltage, as shown in Fig. 6, is longer than that with a step increase of cell voltage.

It can be concluded from the results in Figs. 6 and 7 that heat transfer process and its intricate interactions with the liquid water saturation increase the transient response time of a PEM fuel cell undergoing a step change of cell voltage. This conclusion is consistent with that drawn in [32] calculated using a single-phase model. Fig. 8 illustrates the temperature distributions at different time steps corresponding to the same operation

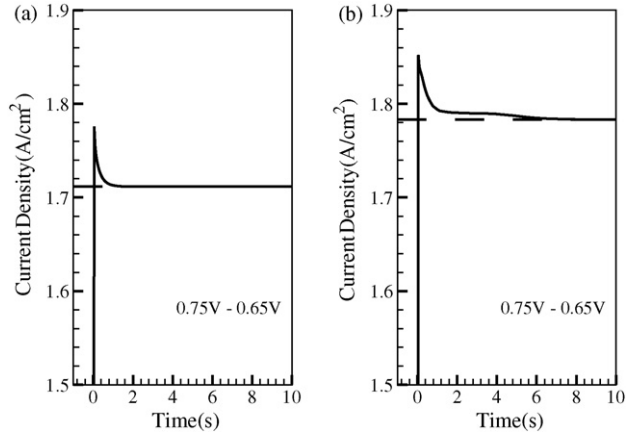

Fig. 6. Transient responses of the fuel cell with a step decrease of cell voltage under two-phase (a) isothermal and (b) non-isothermal conditions.

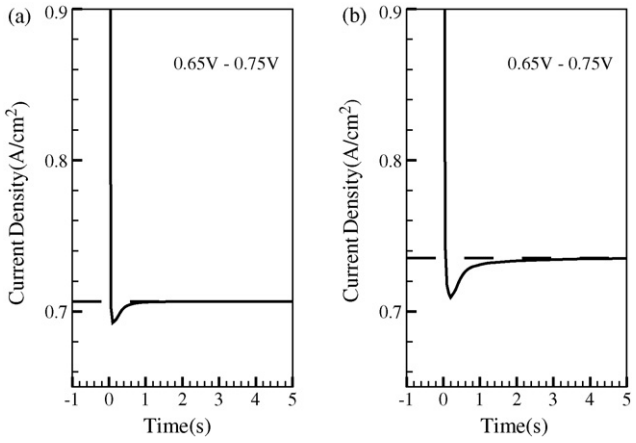

Fig. 7. Transient responses of the fuel cell with a step increase of cell voltage under two-phase (a) isothermal and (b) non-isothermal conditions.

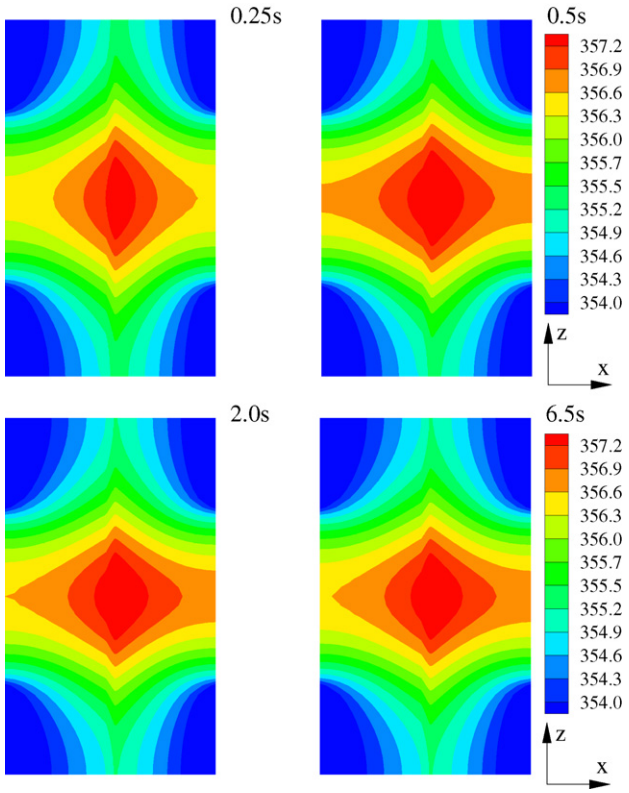

Fig. 8. Transient variations of cell temperature corresponding to the same operation condition as in Fig. 6b.

conditions as in Fig. 6b. Significant temperature variations can be observed from 0 to around 2.0 s on both the anode and cathode sides, consistent with the dramatic variations of the current density shown in Fig. 6b. After 2.0 s, only slight variations of the temperature distribution can be found, also consistent with the small current density variations in Fig. 6b. The temperature variations are closely coupled with the liquid water saturation variations, as shown in Fig. 9. With the temperature increasing, a condensation/evaporation interface appears in the porous materials directly under the gas channel, and a dry region expands with time, especially from 0 to 2.0 s.

The transient variations of temperature and liquid saturation distributions would affect the water content distribution inside the membrane, as shown in Fig. 10. With the increase of the temperature and the appearance of a dry region directly under the gas channel, the water content inside the membrane decreases at the corresponding region, as clearly illustrated in Fig. 10. Therefore, it can be concluded that the heat transfer process influences the transient responses of a fuel cell through its intricate interactions with liquid water saturation in the porous materials and the water content inside the membrane under two-phase non-isothermal conditions, which in turn will affect the electrochemical kinetics, species transport, and membrane hydration/dehydration processes in a PEM fuel cell.

The numerical results presented above are all calculated without considering the liquid droplet coverage phenomenon at the GDL/GC interface. In fact, downstream in the gas channel, with the water vapor oversaturated and the decrease of current density and consequently the decrease of temperature, the condensation/evaporation interface directly under the gas channel would disappear, and as such liquid water will emerge from the GDL and attach at the GDL/GC interface. This phenomenon has been fully examined and discussed in reference [17] for a steady-state two-phase PEM fuel cell simulation. In order to include the

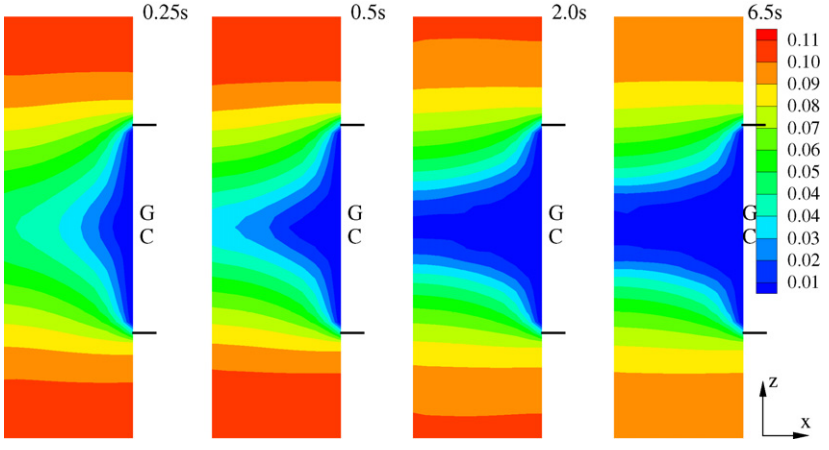

Fig. 9. Transient variations of liquid water saturation in cathode GDL corresponding to the same operation condition as in Fig. 6b.

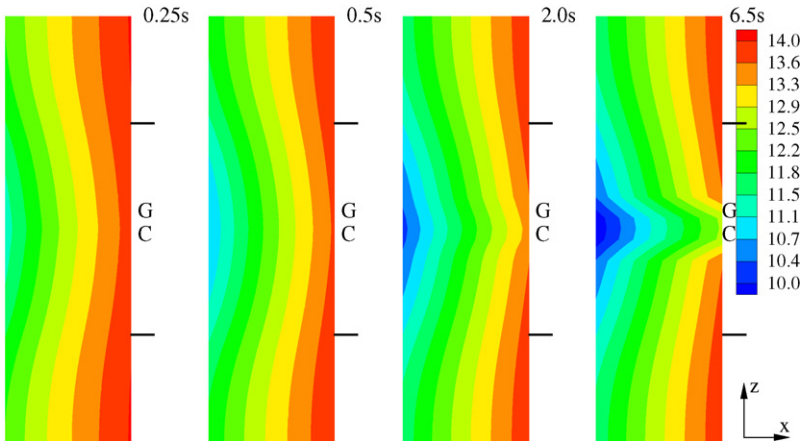

Fig. 10. Transient variations of water content inside the membrane corresponding to the same operation condition as in Fig. 6b.

effects of the liquid droplet coverage on the transient responses of a PEM fuel cell in the present two-dimensional simulations, the heat transfer process is neglected in the following calculations. Fig. 11 compares the transient responses of a PEM fuel cell undergoing a step decrease of cell voltage from 0.75 to 0.65 V under the two-phase isothermal condition with and without the liquid droplet coverage phenomenon. The transient current density variations with a step increase of cell voltage from 0.65 to 0.75 V, with the other operation conditions remaining the same as in Fig. 11, are presented in Fig. 12. In both Figs. 11b and 12b, the liquid saturation values defined at the GDL/GC interface are 0.5 at 0.65 V and 0.3 at 0.75 V, appropriately accounting for the current density effect on the degree of the interfacial liquid droplet coverage. As the liquid droplet coverage at the GDL/GC interface strongly affects the liquid saturation value in the porous materials, it will significantly affect species transport, resulting in drastic over-shoot and under-shoot of the current density corresponding to a step change of cell voltage. The over-shoot of the current density with a step decrease of cell voltage is especially strong, reaching around 20% of the final steady-state value, as shown in Fig. 11b. Both Figs. 11b and 12b indicate that the

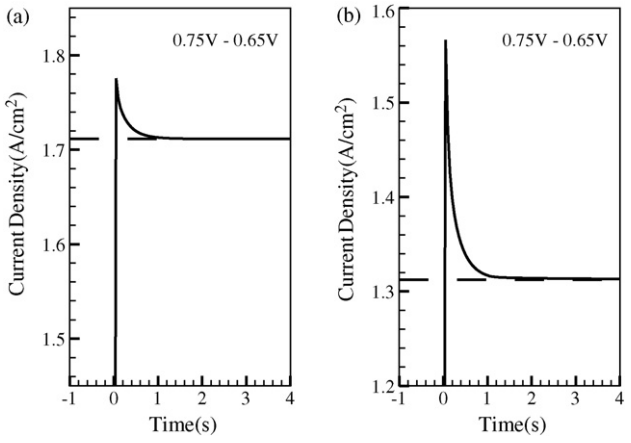

Fig. 11. Transient responses of the fuel cell with a step decrease of cell voltage under isothermal two-phase conditions; (a) without interfacial liquid droplet coverage and (b) with interfacial liquid droplet coverage.

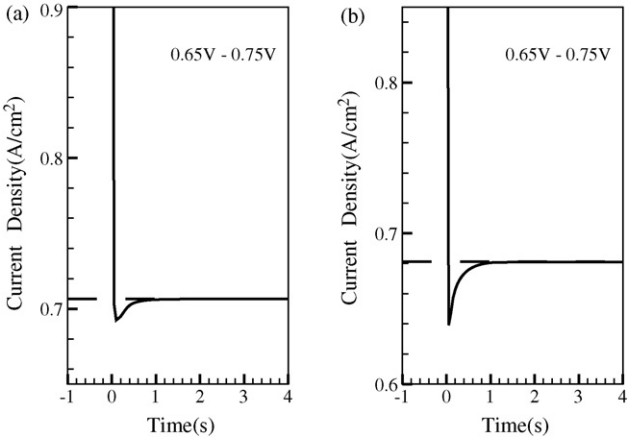

Fig. 12. Transient responses of the fuel cell with a step increase of cell voltage under isothermal two-phase conditions; (a) without interfacial liquid droplet coverage and (b) with interfacial liquid droplet coverage.

effect of the interfacial liquid droplet coverage on the transient response time is negligible. However, it should be emphasized that in the present numerical simulations, the liquid saturation value at the GDL/GC interface has been assumed to change instantly with a step change of cell voltage. In the real-world operations, the interfacial saturation value should vary with time, and therefore, it could exert influences on not only the magnitude but also the time of the transient response process. The transient characteristics of the liquid droplet coverage at the GDL/GC interface should be determined through extensive experiments, and deserves further studies. Based on the present numerical results and discussions, it can be concluded that the effect of the liquid droplet coverage at the GDL/GC interface on the transient response of a PEM fuel cell is extremely strong and thus cannot be neglected in two-phase transient PEM fuel cell simulations.

4. Conclusion

In this paper, a transient two-phase non-isothermal PEM fuel cell model has been developed based on the previously

established two-phase mixed-domain approach. This model is capable of solving two-phase flow and heat transfer processes simultaneously with a proper consideration of the effect of liquid droplet coverage at the gas diffusion layer and the gas channel interface. The model has been applied for two-dimensional time-accurate simulations in a cross-section perpendicular to the flow direction to fully examine the effects of liquid water transport and heat transfer phenomena on the transient responses of a PEM fuel cell undergoing a step change of cell voltage, with and without condensation/evaporation interfaces.

The present numerical results show that under isothermal two-phase conditions, the presence of liquid water in the porous materials increases the current density over-shoot and under-shoot, compared with the results under isothermal single-phase condition. Under the non-isothermal two-phase conditions, the heat transfer process significantly increases the transient response time. The heat transfer process influences the transient responses of a PEM fuel cell through its intricate interactions with liquid water saturation in the porous materials and the water content inside the membrane, which in turn affect the electrochemical kinetics, species transport, and membrane hydration/dehydration processes in the fuel cell.

The present studies also indicate that, with an inclusion of the liquid droplet coverage at the GDL/GC interface, the interfacial liquid saturation level strongly affects the liquid saturation value inside the porous materials, and it in turn significantly influences species transport, resulting in drastic over-shoot and under-shoot of the current density with a step change of cell voltage. In fact, if the transient characteristics of the interfacial liquid droplet coverage could be determined and applied in the simulations, it would exert influences on not only the magnitude but also the time of the transient response process. This phenomenon will be further investigated in the future research work.

Acknowledgements

This work is partially supported by The Ministry of Personnel of PR China and The Department of Personnel of Zhejiang Province (J20070016).

References

[1] S. Um, C.Y. Wang, K.S. Chen, J. Electrochem. Soc. 147 (2000) 4485.
[2] S. Dutta, S. Shimpalee, J.W. Van Zee, Int. J. Heat Mass Transfer 44 (2001) 2029.
[3] N.P. Siegel, M.W. Ellis, D.J. Nelson, M.R. von Spakovsky, J. Power Sources 115 (2003) 81.
[4] S. Mazumder, J.V. Cole, J. Electrochem. Soc. 150 (2003) A1503.
[5] H. Meng, C.Y. Wang, J. Electrochem. Soc. 151 (2004) A358.
[6] H. Meng, C.Y. Wang, Chem. Eng. Sci. 59 (2004) 3331.
[7] H. Ju, H. Meng, C.Y. Wang, Int. J. Heat Mass Transfer 48 (2005) 1303.
[8] B. Hum, X. Li, J. Appl. Electrochem. 34 (2004) 205.
[9] V. Gurau, H. Liu, S. Kakac, AIChE J. 44 (1998) 2410.
[10] T. Berning, D.M. Lu, N. Djilali, J. Power Sources 106 (2002) 284.
[11] B.R. Sivertsen, N. Djilali, J. Power Sources 141 (2005) 65.
[12] H. Meng, J. Power Sources 162 (2006) 426.
[13] H. Meng, J. Power Sources 164 (2007) 688.
[14] Z.H. Wang, C.Y. Wang, K.S. Chen, J. Power Sources 94 (2001) 40.
[15] L. You, H. Liu, Int. J. Heat Mass Transfer 45 (2002) 2277.
[16] S. Mazumder, J.V. Cole, J. Electrochem. Soc. 150 (2003) A1510.
[17] H. Meng, C.Y. Wang, J. Electrochem. Soc. 152 (2005) A1733.
[18] T. Berning, N. Djilali, J. Electrochem. Soc. 150 (2003) A1598.
[19] U. Pasaogullari, C.Y. Wang, J. Electrochem. Soc. 152 (2005) A380.
[20] W. He, J.S. Yi, T.V. Nguyen, AIChE J. 46 (2000) 2053.
[21] D. Natarajan, T.V. Nguyen, J. Electrochem. Soc. 148 (2001) A1324.
[22] G. Lin, T.V. Nguyen, J. Electrochem. Soc. 153 (2006) A372.
[23] W.Q. Tao, C.H. Min, X.L. Liu, Y.L. He, B.H. Yin, W. Jiang, J. Power Sources 160 (2006) 359.
[24] H. Ju, G. Luo, C.Y. Wang, J. Electrochem. Soc. 154 (2007) B218.
[25] G. Luo, H. Ju, C.Y. Wang, J. Electrochem. Soc. 154 (2007) B316.
[26] H. Meng, J. Power Sources 168 (2007) 218.
[27] Y. Wang, C.Y. Wang, Electrochim. Acta 50 (2005) 1307.
[28] Y. Wang, C.Y. Wang, Electrochim. Acta 51 (2006) 3924.
[29] H. Meng, C.Y. Wang, Fuel Cells 5 (2005) 455.
[30] S. Shimpalee, W.K. Lee, J.W. Van Zee, H. Naseri-Neshat, J. Power Sources 156 (2006) 355.
[31] S. Shimpalee, W.K. Lee, J.W. Van Zee, H. Naseri-Neshat, J. Power Sources 156 (2006) 369.
[32] H. Wu, P. Berg, X. Li, J. Power Sources 165 (2007) 232.
[33] H. Wu, X. Li, P. Berg, Int. J. Hydrogen Energy 32 (2007) 2022.
[34] C.Y. Wang, Chem. Rev. 104 (2004) 4727.
[35] A.A. Shah, G.S. Kim, P.C. Sui, D. Harvey, J. Power Sources 163 (2007) 793.
[36] D. Song, Q. Wang, Z.-S. Liu, C. Huang, J. Power Sources 159 (2006) 928.
[37] Y. Wang, C.Y. Wang, J. Electrochem. Soc. 152 (2005) A445.